Available online at www.sciencedirect.com

SCIENCE DIRECT®

Computational Materials Science 32 (2005) 96–106

COMPUTATIONAL MATERIALS SCIENCE

www.elsevier.com/locate/commatsci

The nature of a floating electron

M. Skorobogatiy [a,*], I.J. Park [b], J.D. Joannopoulos [b]

[a] *Ecole Polytechnique de Montreal, Genie Physique, C.P. 6079, succ. Centre-Ville Montreal, QC, Canada H3C3A7*
[b] *Department of Physics and Center for Material Science and Engineering, Massachusetts Institute of Technology, Cambridge, MA 02139, USA*

Received 1 March 2004; accepted 29 April 2004

Abstract

Dynamics of electron solvation at the water surface is studied using extensive ab initio simulations. Calculations have been performed on semi-classical water at 300 K temperature with an excess quantum electron on its surface. It is found that after a very fast 30–50 fs initial localization, there follow fast 50–70 fs rotationally mediated transitions of the excess electron between surface trap states with a lifetime of 150–400 fs. In less then 2 ps the excess electron gets trapped in an ordered "floating" electron state on the surface of water with a lifetime of more than 7 ps. The excess electron diffusion coefficient and spectrum of its velocity autocorrelation function change over time to reflect a transition from a very mobile phase (first 2 ps) to a trapped "floating" electron phase (2–7 ps).

Keywords: Wet electron; Solvated electron; Water surface; Density functional theory

---

1. Introduction

The mechanisms and dynamics of electron solvation and migration in fluids have received considerable attention in a number of experimental and theoretical groups because of their practical and fundamental importance. The interest in this species has been widespread not only because of its intriguing physics but also because of its practical importance in numerous areas of chemistry and technology. The species is ubiquitous in irradiated aqueous systems and in electrochemical reactions. Understanding of such processes as carrier mobility, electron transfer reactions [1], electrochemical processes and chemical reactions in solutions [2], electron solvation in fluids [3,4] and electron attachment and localization on clusters [5,6] rely crucially on our understanding of electron dynamics in fluids on a molecular level. In this study we shall focus on the molecular dynamics of an excess electron interacting with a surface of water.

Because of its very small mass, the electron is an inherently quantum object and some of its properties such as, for example, the diffusion coefficient in bulk water can be explained only by resorting to

---

[*] Corresponding author. Tel.: +1-514-340-4711x3327; fax: +1-514-340-3218.

E-mail address: maksim.skorobogatiy@polymtl.ca (M. Skorobogatiy).

0927-0256/$ - see front matter
doi:10.1016/j.commatsci.2004.04.007

a quantum formulation. Water itself at room temperatures presents a very challenging system for study mainly because the strength of the hydrogen bond is comparable to the thermal energy of fluctuations, thus leading to a very mobile structure of the hydrogen bond network.

An excess electron can be introduced into a neutral water system by several different mechanisms, including radiolysis, electrochemical processes, and optical excitation of water molecules [7]. Currently, only the optical excitation mechanism allows a direct observation of the fast processes in the femtosecond range, during and after the formation of a solvated electron. Thus, most of the experiments in water have been performed on photo-excited aqueous electrons in the bulk of the solvent [8–16]. For the same reason, most of the theoretical [17–25] and theoretical computational [26–50] research efforts so far have concentrated on the study of excess electron solvation dynamics in the bulk of a fluid.

It is known that a solvated electron in water forms a cavity-like structure of approximately 4–6 Å in diameter. An excess electron density in the middle is surrounded by favorably oriented solvent molecules where an excess electron mainly interacts with the hydrogen atoms that are not directly involved in hydrogen bonding with other water molecules. It is also known that diffusion coefficient [44,50] of excess electron in water is almost twice as high as that one of surrounding water which is attributed to the quantum nature of the excess electron.

Generally, it is assumed that an excess electron appears instantaneously in the bulk of water and further dynamics is described from such a point in time. This scenario is indeed possible when an electron is photo-excited in the bulk of water by a laser. However, if the surface of the water is located nearby a photo-excited electron or if an excess electron is injected into the water by an outside source, the dynamics of solvation of such an electron will be influenced by this surface. Original work on solvation of an excess electron on the surface of water clusters have been done by [29,33,35,36,38]. It was established that for large clusters (more than 64 water molecules) excess electron has a slightly lower free energy inside the water cluster than on the cluster surface. Starting with medium cluster sizes (256 water molecules) a long living surface state emerges with a lifetime of more than 1 ps.

The aim of this paper is to investigate the long term (beyond 1 ps) dynamics of electron solvation when the water surface, rather than a cluster surface, is present and to explore the nature of a possible "floating" electron state.

The work is presented in the following order. In Section 2 we describe the classical flexible water model and molecular pseudopotentials for the interaction with an excess electron. The initial stage of an excess electron localization (0–200 fs) on the surface of water is considered in Section 3. The intermediate regime of electron solvation (200 fs–2 ps) including the nature of the traps and inter-trap transitions, is addressed in Section 3.1. In this section, the dynamics of excess electron solvation including the excess electron spacial trajectory, excess electron–water diffusion coefficient and spectral density of excess electron autocorrelation function are discussed. In Section 3.2 we discuss the structure of a fully developed surface state. Finally, in Section 4 we make some concluding remarks.

2. Classical water and quantum excess electron simulations

To study excess electron dynamics in water one has to account for the electron's quantum nature. Ideally, the water itself should be described quantum mechanically. In practice, because of the hundreds of water molecules involved in a simulation and the multiple valence electrons on each water molecule, the quantum description of water becomes problematic. Thus, we model an excess electron using a density functional theory approach, with the solvent treated using a classical polarizable water model, and the interactions between the quantum electron and classical water treated through the use of molecular pseudopotentials.

For a normal density of water 1.0 g/cm^3 at $T = 300$ K, 112 molecules will occupy a box of (15 Å,15 Å,15 Å). To simulate a surface of water we choose a simulation box twice as large in the vertical direction (15 Å,15 Å, 30 Å) while still maintaining 112 molecules. Interatomic interactions in this model are introduced via a flexible water molecule potential in which inter-molecule and intra-molecule potentials are fitted to ab initio data [50].

To maximize the amount of vacuum above the water surface (which will be very important when a quantum electron is placed on top) we constrain the first two layers (20 molecules) of the water molecules to move around their ice-like positions. The constraint is implemented via an effective "spring" where one end is attached to the oxygen atom of a corresponding water molecule and the other end is attached to the proper ice-like lattice position in space. Also, to minimize the net dipole moment of these two "thermostat" layers in the vertical direction, we constrain the dipoles of these molecules to lie predominantly in the horizontal plane. This constraint is implemented by means of effective one dimensional "springs" along the vertical direction where one end is connected to the corresponding hydrogen atoms of the water molecule while the other end is in the horizontal plane going through the oxygen atom of the same water molecule. A thermostat is imposed through the rescaling of the velocities of the molecules in these two layers. The rest of the molecules are allowed to move freely. After a 100 ps thermalization run without an excess electron, equilibrium is achieved. In equilibrium, 7 Å are taken by the thermostat, 14 Å are taken by the bulk and surface and the rest 9 Å is vacuum. Two equilibrium "realizations" of the water surface are taken to be the starting point of the excess electron solvation simulations.

To make sure our system is not biased toward a surface state, we also run a simulation of an excess electron in the "bulk" region of our cell. For that we first fix 6 water molecules in a Kevan cavity geometry without an excess electron in it. The Kevan cavity is placed in the "bulk" region of the simulation cell and allowed to equilibrate for 100 ps. We then introduce the excess electron and then follow its dynamic evolution quantum mechanically.

2.1. Classical polarizable water model

To correctly model equilibrium water properties, important features such as water molecule geometry, dipole moments, hydrogen bond energies, etc. must be correctly reproduced by the interaction potentials. Incorporation of internal degrees of freedom of a water molecule such as vibrational excitations can be very important when dealing with dynamic processes. For the problem of an excess electron diffusing in water it was recognized [42,20] that vibrational degrees of freedom play an important role providing an additional mechanism for the coupling of the electron energy to the thermostat.

In our work, we use an ab initio fitted flexible water–water interaction potential [51]. The potential energy between two flexible water molecules can be written as a sum of two contributions arising from inter-molecular and intra-molecular motions

$$V(r_{\alpha,\beta}, \delta_i) = V_{\text{inter}}(r_{\alpha,\beta}) + V_{\text{intra}}(\delta_i) \quad (1)$$

where $r_{\alpha,\beta}$ are the inter-molecular atomic distances, and δ_i are the internal coordinates. The inter-molecular potential is ab initio fitted to reproduce the correct energies and geometries of the hydrogen bonded dimer. The intra-molecular potential is also ab initio fitted to reproduce frequencies of molecular stretching and bending modes.

The equilibrium bond length R_e and bond angle θ_e predicted from the theoretical calculations are 0.9576 Å and 104.59, respectively, to be compared with the experimental values of 0.9572 Å and 104.52. As the M center does not reside on any atom, in the case of the flexible water model, we restrict M to be on the line bisecting the H–O–H angle and the ratio $r_{\text{OM}}/r_{\text{OM}'}$ is taken to be a constant, equal to the 0.456826. With this potential it is found that the binding energy between two molecules is −5.94 kcal/mol with 0.07 kcal/mol coming from the intra-molecular potential.

Periodic boundary conditions are applied to the computational cell. To avoid spurious self-interactions between water molecules we use a cutoff radius $R_c = 7.5$ Å and a reaction field method where the properties of the thermostat beyond the cutoff radius are approximated and included as a correction to an interaction potential [52–54].

As we specified before we used 112 water molecules in the (15 Å, 15 Å, 30 Å) computational cell. Water was first equilibrated over a very long, 100 ps, equilibration run with a consequent 20 ps period during which statistics was gathered. After equilibration 7 Å of the the thermostat region, 9 Å of the bulk region of almost constant density of 0.8 g/cm^3 and a 5 Å of the surface region where the value of the density drops from its bulk value to almost zero could be clearly identified. Thus, after equilibration the computational cell is subdivided into bulk-like (~9 Å) and surface-like (~5 Å) regions with a vacuum region (~9 Å) separating the water surface and the thermostat. We also computed the self-diffusion coefficient of water in the different regions of the computational cell. In the bulk region, the self diffusion coefficient of water has values in the range $1.0–3.0\times10^{-5}$ cm^2/s which is around the accepted value 2.4×10^{-5} cm^2/s of the bulk self-diffusion coefficient of water at 300 K. In the surface region, however, the self diffusion coefficient has values averaging around 4.2×10^{-5} cm^2/s which is almost twice as large as the corresponding bulk value. Thus the dynamics of water molecules on the surface is significantly faster than in the bulk.

2.2. Quantum electron—classical water interaction, molecular pseudopotentials

In our simulations we use density functional theory to model the ground state density and energy of an excess quantum electron.

Interaction between a quantum excess electron and classical water molecules is modeled via the molecular pseudopotentials. While ionic pseudopotentials describe the field in which valence electrons interact with the core of an atom, molecular pseudopotentials describe the field in which valence electrons interact with a neutral molecule. We obtain molecular pseudopotentials by the fitting a physically motivated form for such a potential to the ab initio density functional calculations of the wavefunction and energy associated with an excess electron in an isolated molecule described by ionic pseudopotentials.

The field of construction of molecular pseudopotentials is very broad and important by itself. There have been numerous electron–water molecular pseudopotentials suggested in the literature [28,29,32,55] all based on the same set of underlying physical ideas. In the following we adopt the same molecular pseudopotentials as in [50]. One starts with defining major physically motivated contributions to the potentials. These are the Coulomb, polarization, exclusion and exchange contributions

$$V(r_e, R_O, R_{H1}, R_{H2}) = V_{coul} + V_p + V_{e,x} \tag{2}$$

where r_e is the position of an excess electron, and R_O, R_{H1}, R_{H2} are the positions of the oxygen and hydrogen atoms of a water molecule. The coulomb contribution is constructed to reproduce the equilibrium dipole moment of a water molecule. The polarization contribution to the molecular potential describes the polarizability of the molecular valence cloud in an excess field of an excess electron. It is taken to be similar to the adiabatic polarization potential that can be derived from standard perturbation theory of a molecule with a permanent dipole [56]. The exclusion contribution to the potential reflects the fact that there is a repulsion between an excess electron and the water molecule at small distances due to the orthogonality of the wave function of an excess electron to the wave function of the valence electrons of the water molecule. The exchange contribution reflects the antisymmetric nature of the total wave function. The exclusion-exchange term also removes singularity in the electrostatic potential at the atomic centers.

All the parameters were successfully tested to predict the corresponding properties of an ab initio water dimer. Two dimer calculations were actually performed. In the first calculation, both water molecules were described in terms of ionic pseudopotentials. In the second calculation, one of the water molecules is described in terms of the molecular pseudopotentials. It was found that the molecular pseudopotential can accurately reproduce the excess electron distribution, not only for static case, but also for the case of room temperature vibrational motions within 6%.

3. Initial localization of the electron cloud

To make the visualization of the electron density distribution in the computational cell more objective we shift all the molecules along the vertical direction so that the vacuum region is located in the middle of the computational cell. In the upper edge of the vacuum region (left panel in Fig. 1) one finds the two layers of the thermostat and a part of the "bulk" water, while the less dense and substantially more rugged surface of water is located in the lower part of the vacuum region.

When an excess electron is introduced into a system before any structural relaxations of the water, the electron becomes trapped into one of the very delocalized surface states with mean square radius 4–6 Å. As one can see from Fig. 1, in the next 30–60 fs a very fast localization occurs with radius of the electron cloud shrinking to its equilibrium value of ~1.8 Å. This localization is driven by rotational motions of the water molecules around the localized electron. Since the rotational time scale is ~50 fs, the water molecules around an excess electron reorient themselves on the order of this time-scale to make new hydrogen-bonds with the electron cloud. In the following 150 fs, the total electron and water energy drops halfway to its equilibrium value signifying a formation of an initial solvation shell around the electron cloud. Further energy relaxation is much slower and does not simply constitute the relaxation of this primary solvation shell as might be expected. This is demonstrated in detail in the next section.

3.1. Dynamics of the "floating" excess electron on the water surface

After initial fast localization, the excess electron begins to explore the surface of water. In Fig. 2, we plot the excess electron trajectory for a 309 K "surface" run during the first 2 ps. These results reveal that early diffusion of an electron cloud on the surface of water proceeds through relatively long lived (150–400 fs) trap states (placed in dotted circles on Fig. 2) connected by the inter-trap

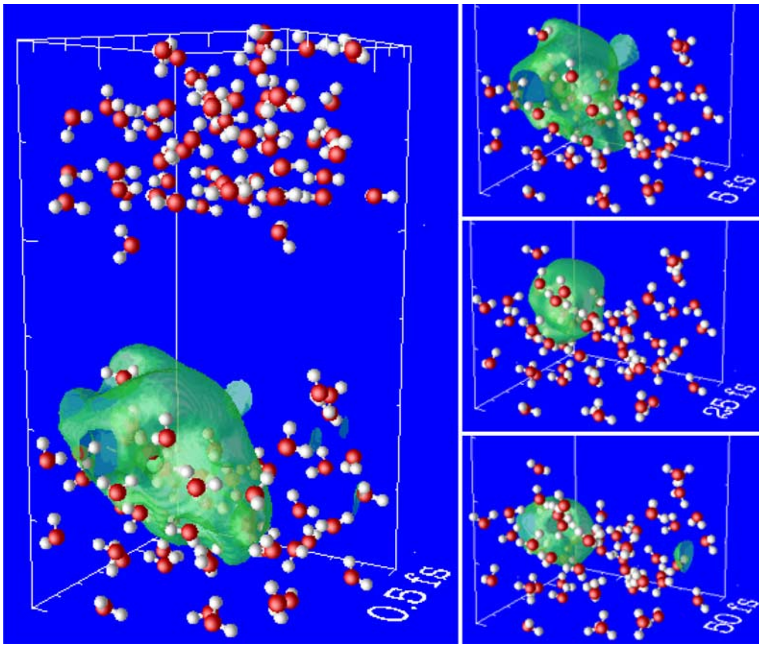

Fig. 1. Snapshots of the electron density cloud during the first 50 fs of the electron localization on a surface of classical water. There is almost no translational motion of the water molecules to be seen on this timescale, however rotational motions of the water molecules are clearly visible. Initial localization, thus, is mostly driven by molecular rotations with a characteristic timescale of 30–50 fs.

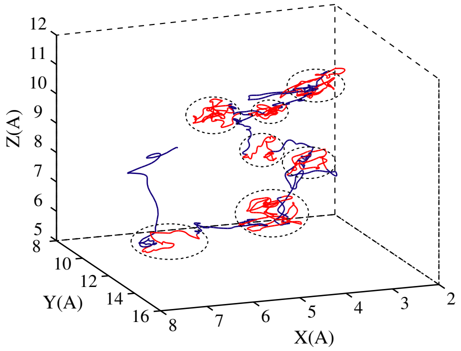

Fig. 2. Excess electron trajectory during the first 2 ps of a 309 K "surface" run. Water surface is located in between 6–10 Å. In dotted circles we highlight the trap regions along the trajectory, which are connected by the inter-trap transition regions.

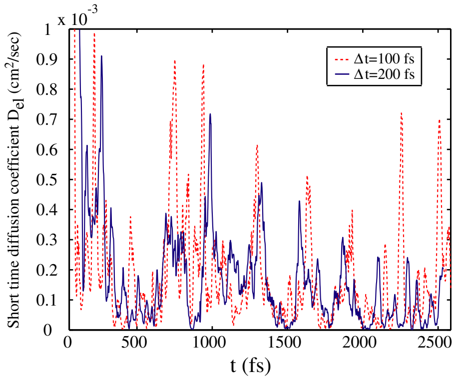

Fig. 3. Short time diffusion coefficients during the first 2 ps of the 309 K "surface" run. Peaks on the plots correspond to the fast inter-trap transition regions while the shallow inter-peak regions correspond to the traps.

transitions regions with very fast inter-trap transition times (50–70 fs) being on the time scale of rotations of the water molecules.

One way of defining the trap regions is by plotting a short time diffusion coefficient at each point of time t along the excess electron trajectory. Such a diffusion coefficient defines the short time dynamics of an excess electron and provides a consistent way of characterizing local electron dynamics over the relevant range of time periods Δt. We calculate excess electron diffusion coefficient as

$$D_{\mathrm{el}}(t,\Delta t) = \frac{1}{6\Delta t} < (r(t+\Delta t) - r(t))^2 >, \tag{3}$$

where Δt is on the order of a lifetime of a trap and averaging is performed at each time step over the following time interval of $\sim \Delta t$. In Fig. 3 short time diffusion coefficients are plotted for different values of $\Delta t \in$[100, 200 fs]. High excess electron mobility regions (peaks on the Fig. 3 plots) correspond to the fast inter-trap transition regions while the shallow inter-peak regions correspond to the traps. We have established that positions of the traps are consistent for the averaging times $\Delta t \sim$100–300 fs. We have also established that traps defined by the shallow inter-peak regions of Fig. 3 coincide well with the traps defined visually from the Fig. 2. Analysis of the 291 K "surface" run leads to similar conclusions on the excess electron dynamics during the first 2 ps period.

During the same initial period "bulk" run shows localization of the excess electron in the "bulk" region of the cell. Center of the electron density fluctuates along the vertical direction with an amplitude of approximately 1 Å. The "bulk" excess electron energy and the structure of the "wet" water shell around it is remarkably similar to that of the "surface" excess electron.

Next, we explore the long time diffusion coefficient of an excess electron on the surface of water. For this purpose we use the same expression (3) with $\Delta t = 1$ ps. The long time diffusion coefficient of an excess electron is plotted on Fig. 4 as a function of time. As formation of the "floating" electron is a non-equilibrium process one expects the long time diffusion coefficient to vary along with formation of a stable surface state. Fig. 4 shows that in the first 1–2 ps, the excess electron exhibits a very large mobility with diffusion coefficient on the order of $10.0\text{–}30.0 \times 10^{-5}$ cm^{-5} cm^2/s which is 2–6 times larger than the self-diffusion coefficient of a solvated electron in the bulk. This is because in the the first several picoseconds the stable water shell around the excess electron is formed mostly by fast rotations of water dipoles rather than by slow translational motions of water molecules. Thus, the electron gets frequently (200–400 fs, Figs. 2 and 3) exchanged between abundant spatially separated energetic minima (traps), contributing to its large mobility. After 2 ps, a

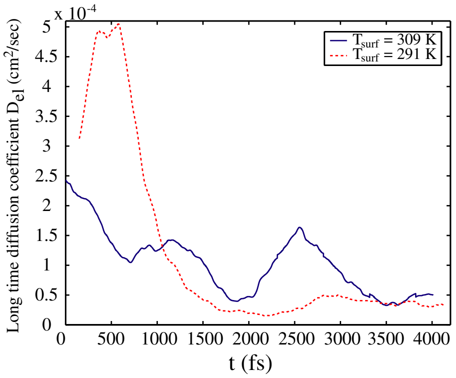

Fig. 4. Long time diffusion coefficients along the excess electron trajectory. Initial high excess electron mobility in "surface" runs, is attributed to the frequent inter-trap transitions initiated by the rotations of water dipoles. Subsequent reduction in the excess electron mobility is attributed to the formation of a stable water shell around the "floating" electron, making its surrounding "bulk"-like.

well-structured water shell is formed around the excess electron with a substantial energetic barrier for a transition to a nearby competing trap. Thus, the mobility of an excess "floating" electron on a surface is reduced, and its diffusion coefficient becomes comparable that of a "bulk" solvated electron 5.0×10^{-5} cm^2/s.

To demonstrate competition between the potential electron traps and to investigate further the nature of the inter-trap transitions during the first several picoseconds of the excess electron solvation, we present snapshots of the excess electron density distribution for one such inter-trap transition attempt in Fig. 5. At 580 fs, due to thermal fluctuations, there is an alternative trap formed (circled in Fig. 5) nearby the electron cloud. Between 595 and 605 fs, we find that one of the water molecules try to minimize its energy by forming a proper hydrogen bond with another water molecule. Such a molecule starts rotating, leading (as we find from analysis of the corresponding energies) to a decrease of the solvent energy by an amount of the hydrogen bond energy. This, in turn, pulls the excess electron cloud into the new trap. However, judging by the total energy of the system, the new trap happens to be substantially less energetically favorable and the electron density gets pulled back into its original trap. Finally,

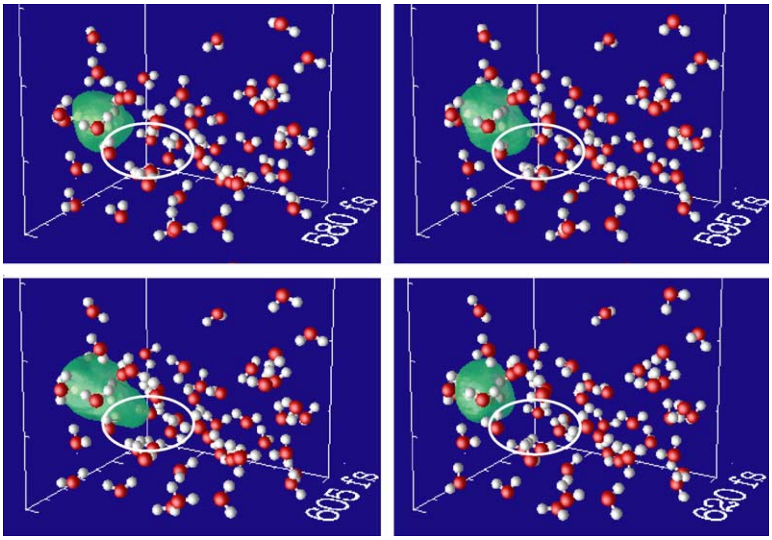

Fig. 5. Snapshots of excess electron–water configurations during a typical transition attempt. Due to thermal fluctuations an alternative trap (circled) is formed nearby the excess electron at 580 fs. Due to the rotation of a water molecule trying to establish a proper hydrogen bond with another molecule, excess electron density begins to get pulled into the new trap. This is clearly visible at 595 and 605 fs. However, the new trap happens to be too energetically unfavorable and the excess electron density is pulled back into the original trap.

we find that the water molecule that initiated the process also rotates back into its original position at 620 fs.

Dynamics of water molecules surrounding the excess electron also play an important role in the formation and dynamics of electron traps. In particular, it is of interest to consider what excitations of water molecules contribute strongly to the electron dynamics. As the position of the center of mass of an excess electron cloud will be strongly affected by the motion of surrounding water molecules, we use the excess electron velocity autocorrelation function (VACF) to estimate coupling to the molecular degrees of freedom. In Fig. 6 we show spectral densities of the VACF of the center of mass of excess electron $\phi(\omega)$ defined at time t_0 as

$$\phi(\omega, t_0) = \int_{t_0}^{\infty} \mathrm{d}t < v(t_0)v(t) > \exp(\mathrm{i}\omega(t - t_0)). \tag{4}$$

where $v(t)$ is the velocity of the center of mass of the electron cloud at time t. Averages are taken at each t_0 over the following time interval of ~1 ps. In equilibrium, $\phi(\omega, t_0)$ becomes only a function of ω and is the same for any t_0. Integrals over the peaks in the spectral density of VACF correspond to the relative amount of energy in the corresponding exited modes. From the top to bottom we show spectral densities of the VACF for the two "surface" runs and a "bulk" run. Fig. 6(a) and (c) correspond to the first 2 ps and Fig. 6(b) and (d) correspond to the (2–6 ps) of the "floating" electron localization on the water surface. Plots are subdivided into different spectral regions by dashed lines. Spectral peaks in each region correspond to different groups of excited modes. Relative amounts of energy in such groups are reflected by the numbers showed in the corresponding regions.

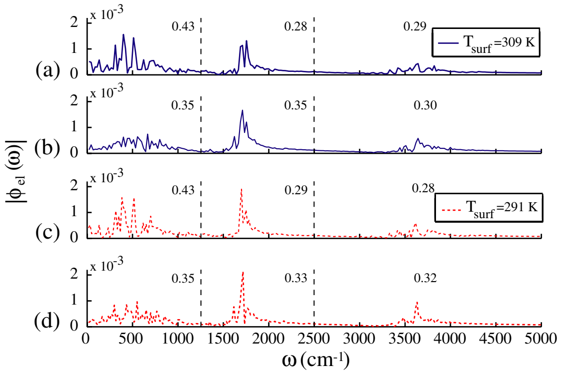

Fig. 6. Spectral density of the excess electron center of mass VACF. Numbers in each region reflect the relative energies in the corresponding excited modes. (a) $t \in (0\ \text{ps}, 2\ \text{ps})$, 309 K "surface" run, (b) $t \in (2\ \text{ps}, 6\ \text{ps})$, 309 K "surface" run, (c) $t \in (0\ \text{ps}, 2\ \text{ps})$, 291 K "surface" run, (d) $t \in (2\ \text{ps}, 6\ \text{ps})$, 291 K "surface" run.

There are several prominent peaks in the VACF spectra of an excess electron common to all the cases of Fig. 6. First, the broad peak around 200–300 cm^{-1} corresponds to the hindered translational motions of the water molecules. The relatively sharp peak at ~500 cm^{-1} corresponds to the rotational motions of the water molecules. A prominent peak at ~1700 cm^{-1} is due to the water intra-molecular bending mode. Finally, the two broad merged peaks around ~3600 cm^{-1} correspond to the water intra-molecular stretching modes.

Comparing spectral densities of the VACF for the initial stage of water shell formation around an excess electron Fig. 6(a) and (c) with these of the later stage of the "floating" electron formation Fig. 6(b) and (d) we find a common trend of increased relative energy in the hindered translational and rotational motions of the water molecules at the beginning of electron localization with a subsequent increase in the bending and stretching modes of water molecules at the later time. This again suggests that the initial dynamics of "floating" electron formation is dominated by water dipole rotations and inter-trap excess electron transitions followed by the final slow, translation-driven, relaxation of the water shell around the "floating" electron.

3.2. Surface state

In Fig. 7, we plot excess electron densities at 2, 3 and 7 ps. We observe that after ~2 ps a surface state is already clearly visible with an irregular shell of water molecules surrounding the excess electron. After ~3 ps an ordered one layer "wet" shell of water molecules is formed. As we follow

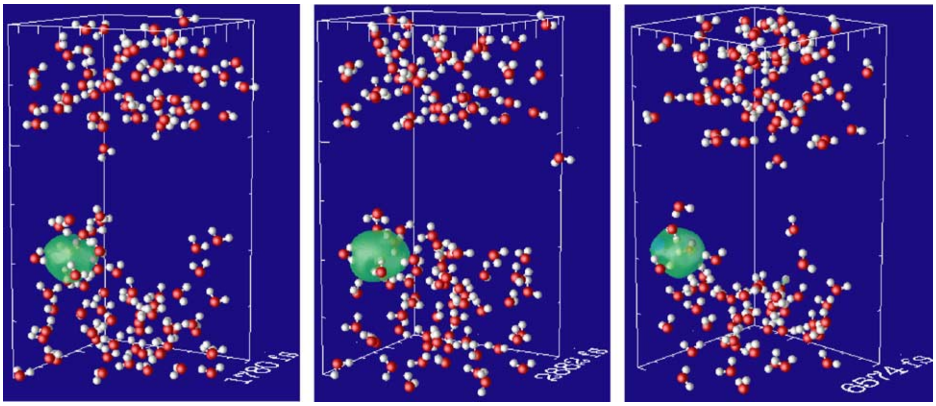

Fig. 7. Surface state of an excess electron after ∼ 2 ps, ∼3 ps and ∼7 ps 309 K "surface" run. At ∼ 2 ps a surface state is clearly visible with an irregular shell of water molecules surrounding an excess electron. After ∼3 ps ordered one layer "wet" shell of water molecules is formed. At 7 ps a very ordered thin "wet" shell surrounds excess electron. At this point electron size, structure and energy are close to that of a totally hydrated electron in the bulk.

the excess electron dynamics in time we observe that even after 7 ps from initial injection, the electron is still bound to the water surface with an ordered one layer "wet" shell surrounding an excess electron. The electron size, structure and energy are all close to a totally hydrated electron in the bulk. This similarity of the fully formed "floating" excess electron to the fully hydrated excess electron apparently is the major factor in slowing the dynamics of the "floating" electron solvation into the bulk. Moreover, the fact that the diffusion coefficient of water molecules on the surface is at least twice as high as the diffusion coefficient of water molecules in the bulk, makes the surface state even more robust, as molecules on a surface can adjust themselves faster to locally trap an excess electron.

4. Concluding remarks

Our microscopic dynamical calculations suggest that a "floating" electron has a lifetime of at least 5 ps. To explore timescales beyond this with the current supercell becomes tricky as molecules evaporate and transverse the computational cell attaching themselves in unrealistic fashion to the surface of the thermostat. We expect that the final solvation of the electron into the bulk, if it eventually happens, must occur on the hydrodynamic time scale. Thus, we can employ a hydrodynamic model to obtain an estimate of this lifetime approaching the problem from a more macroscopic point of view. From the point of view of conventional hydrodynamics, disappearance of a surface state would be initiated by the forces of surface tension on a surface of the shell surrounding excess electron and slowed down by the finite viscosity of water. We estimate the surface state lifetime to be $t = \frac{R\eta}{\sigma}$, where η is a viscosity constant of water, σ is a coefficient of surface tension of water, and R is a characteristic size of a surface state. At $T = 293$ K, $\eta = 1.0019 \times 10^{-3}$ kg/m s, $\sigma = 7.28 \times 10^{-2}$ kg/s^2, and $R = 4$ Å, leading to an estimated lower bound of the "floating" excess electron lifetime of $t \sim 5$ ps. Thus, both microscopic and macroscopic models appear to be consistent with a "floating" electron lifetime that is on the order of tens of ps.

References

[1] M. Armbuster, H. Haberland, H.G. Schindler, Phys. Rev. Lett. 47 (1981) 323.
[2] H. Haberland, H. Langosch, H.G. Schindler, D.R. Worsnop, Surf. Sci. 156 (1985) 517.
[3] M. Knapp, O. Echt, D. Kreisle, E. Recknagel, J. Chem. Phys. 85 (1986) 636.
[4] J.P. Mayer, S.T. Arnold, J.G. Eaton, D. Patel-Misra, H.W. Sarkas, K.H. Bowen (Eds.), Ion Cluster Spectroscopy and Structure, Elsevier, New York, 1989.

[5] G. Benedek, T.P. Martin, G. Pacchioni (Eds.), Articles in Elemental and Molecular Clusters, Springer-Verlag, Berlin, 1988.

[6] T.P. Martin, Phys. Rep. 95 (1983) 167.

[7] A. Bernas, C. Ferradini, J.P. Jay-Gerin, Can. J. Chem. 74 (1996) 1.

[8] A. Migus, Y. Gauduel, J.L. Martin, A. Antonetti, Phys. Rev. Lett. 58 (1987) 1559.

[9] F.H. Long, H. Lu, K.B. Eisenthal, Phys. Rev. Lett. 64 (1990) 1469.

[10] K.H. Schmidt, P. Han, D.M. Bartels, Temperature dependence of solvated electron diffusion in H_2O and D_2O, J. Phys. Chem. 96 (1992) 199.

[11] J.C. Alfano, P.K. Walhout, Y. Kimura, P. Barbara, Ultrafast transient-absorption spectroscopy of the aqueous solvated electron, J. Chem. Phys. 98 (1993) 5996.

[12] J.L. McGowen, H.M. Ajo, J.Z. Zhang, J.Z. Schwartz, Chem. Phys. Lett. 231 (1994) 504.

[13] X.L. Shi, F.H. Long, H. Lu, K.B. Eisenthal, J. Phys. Chem. (1996) 11903.

[14] A. Reuther, A. Laubereau, D.N. Nikogosyan, J. Phys. Chem. 100 (1996) 16795.

[15] M. Assel, R. Laenen, A. Laubereau, Retrapping and solvation dynamics after femtosecond uv excitation of the solvated electron in water, J. Chem. Phys. 111 (1999) 6869.

[16] D. Madsen, C.L. Thomsen, J. Thogersen, S.R. Keiding, Temperature dependent relaxation and recombination dynamics of the hydrated electron, J. Chem. Phys. 113 (2000) 1126.

[17] M. Hilczer, W.M. Bartczak, A statistical model of the solvated electron in polar media, the point-dipole approximation, J. Phys. Chem. 94 (1990) 6165.

[18] S. Golden, T.R. Tuttle Jr., Entropies of solvation of solvated electrons, J. Phys. Chem. 95 (1991) 4109.

[19] J. Zhu, R.I. Cukier, A mean-field theory of a localized excess electron in a polar fluid, J. Chem. Phys. 99 (1993) 5384.

[20] Y.J. Chang, E.W. Castner Jr., Fast responces from slowly relaxing liquids: a comparative study of the femtosecond dynamics of triacetin, ethylene glycol, and water, J. Chem. Phys. 99 (1993) 7289.

[21] I. Rips, Electron solvation dynamics in polar liquids, Chem. Phys. Lett. 245 (1995) 79.

[22] P. Graf, A. Nitzan, G.H.F. Diercksen, Phenomenology of electron solvation in polar fluids, J. Phys. Chem. 100 (1996) 18916.

[23] I. Rips, Cavitation model of electron solvation dynamics: effect of energy dissipation, J. Chem. Phys. 106 (1997) 2702.

[24] A.I. Burshtein, S.G. Fedorenko, Hopping reactions of charged particles, J. Chem. Phys. 106 (1997) 2662.

[25] I. Rips, M. Tachiya, Equilibrium properties of the solvated electron in polar liquids: finite solvent size effects, J. Chem. Phys. 107 (1997) 3924.

[26] M.D. Newton, The role of ab initio calculations in elucidating the properties of hydrated and ammoniated electrons, J. Chem. Phys. 79 (1975) 2795.

[27] J. Schnitker, P.J. Rossky, G.A. Kenney-Wallace, Electron localization in liquid water: A computer simulation of microscopic trapping sites, J. Chem. Phys. 85 (1986) 2986.

[28] A. Wallqvist, G. Martyna, B.J. Berne, Behavior of the hydrated electron at different temperatures: structure and absorption spectrum, J. Phys. Chem. 92 (1988) 1721.

[29] R.N. Barnett, U. Landman, C.L. Cleveland, Surface states of excess electrons on water clusters, Phys. Rev. Lett. 59 (1987) 811.

[30] J. Schnitker, P.J. Rossky, Quantum simulation of the hydrated electron, J. Chem. Phys. 86 (1987) 3471.

[31] P.J. Rossky, J. Schnitker, The hydrated electron: quantum simulation of structure, spectroscopy, and dynamics, J. Chem. Phys. 92 (1988) 4277.

[32] R.N. Barnett, U. Landman, C.L. Cleveland, J. Jortner, Electron localization in water clusters. i. electron–water pseudopotential, J. Chem. Phys. 88 (1988) 4421.

[33] R.N. Barnett, U. Landman, C.L. Cleveland, J. Jortner, Electron localization in water clusters. ii. surface and internal states, J. Chem. Phys. 88 (1988) 4429.

[34] R.N. Barnett, U. Landman, A. Nitzan, Relaxation dynamics following transition of solvated electrons, J. Chem. Phys. 90 (1989) 4413.

[35] R.N. Barnett, U. Landman, A. Nitzan, Dynamics of excess electron migration, solvation, and spectra in polar molecular clusters, J. Chem. Phys. 91 (1989) 5567.

[36] R.N. Barnett, U. Landman, G. Makov, A. Nitzan, Theoretical studies of the spectroscopy of excess electrons in water clusters, J. Chem. Phys. 93 (1990) 6226.

[37] R.N. Barnett, U. Landman, A. Nitzan, Excess electron transport in water, J. Chem. Phys. 93 (1990) 8187.

[38] R.N. Barnett, U. Landman, G. Rajagopal, A. Nitzan, Dynamics, spectra, relaxation phenomena of excess electrons in clusters, Isr. J. Chem. 30 (1990) 85.

[39] F.J. Webster, J. Schnitker, M.S. Fredrichs, R.A. Friesner, P.J. Rossky, Solvation dynamics of the hydrated electron: a nonadiabatic quantum simulation, Phys. Rev. Lett. 66 (1991) 3172.

[40] E. Neria, A. Nitzan, R.N. Barnett, U. Landman, Quantum dynamical simulations of nonadiabatic process: solvation dynamics of the hydrated electron, Phys. Rev. Lett. 67 (1991) 1011.

[41] E. Keszei, S. Nagy, T.H. Murphrey, P.J. Rossky, Kinetic analysis of computer experiments on electron hydration dynamics, J. Chem. Phys. 99 (1993) 2004.

[42] T.H. Murphrey, P.J. Rossky, The role of solvent intramolecular modes in excess electron solvation dynamcis, J. Chem. Phys. 99 (1993) 515.

[43] B.J. Schwartz, P.J. Rossky, Aqueous dynamics with a quantum mechanical solute: computer simulation studies of the photoexcited hydrated electron, J. Chem. Phys. 101 (1994) 6902.

[44] K.S. Kim, I. Park, S. Lee, K. Cho, J.Y. Lee, J. Kim, J.D. Joannopoulos, The nature of a wet electron, Phys. Rev. Lett. 76 (1996) 956.

[45] S. Lee, J. Kim, S.J. Lee, K.S. Kim, Novel structures for the excess electron state of the water hexamer and the

interaction forces governing the structures, Phys. Rev. Lett. 79 (1997) 2038.

[46] K. Drukker, S.W. de Leeuw, Molecular dynamics of an excess electron in aqueous solutions, Chem. Phys. Lett. 291 (1998) 283.

[47] A.A Mosyak, O.V. Prezhdo, P.J. Rossky, Solvation dynamics of an excess electron in methanol and water, J. Chem. Phys. 109 (1998) 6390.

[48] P. Minary, L. Turi, Nonadiabatic molecular dynamics simulation of photoexcitation experiments for the solvated electron in methanol, J. Chem. Phys. 110 (1999) 10953.

[49] S.B. Suh, J. Kim, K.S. Kim, Water dimer to pentamer with an excess electron: ab initio study, J. Chem. Phys. 111 (1999) 10077.

[50] I. Park, K. Cho, S. Lee, K.S. Kim, J.D. Joannopoulos, Ab initio atomistic dynamical study of an excess electron in water, Comp. Mater. Sci. 21 (2001) 291.

[51] G.C. Lie, E. Clementi, Molecular-dynamics simulation of liquid water with an ab initio flexible water–water interaction potential, Phys. Rev. A 33 (1986) 2679.

[52] W.F. van Gunsteren, H.J.C. Berendsen, J.A.C. Rullmann, Inclusion of reaction fields in molecular dynamics: application to liquid water, Discuss. Faraday Soc. 66 (1978) 58.

[53] I.G. Tironi, B.A. Luty, W.F. van Gunsteren, Space-time correlated reaction field: a stochastic dynamical approach to the dielectric continuum, J. Chem. Phys. 106 (1997) 6068.

[54] D. van der Spoel, P.J. van Maaren, Herman J.C. Berendsen, A systematic study of water models for molecular simulation: Derivation of water models optimized for use with a reaction field, J. Chem. Phys. 108 (1998) 10220.

[55] J. Schnitker, P.J. Rossky, An electron–water pseudopotential for condensed phase simulation, J. Chem. Phys. 86 (1987) 3462.

[56] C.H. Douglas, D.A. Weil, P.A. Charlier, R.A. Eades, D.G. Truhlar, D.A. Dixon, Chemical Applications of Atomic and Molecular Electrostatic Potentials, Plenum, New York, 1981.